Gallagher, S.J., Fulthorpe, C.S., Bogus, K., and the Expedition 356 Scientists
Proceedings of the International Ocean Discovery Program Volume 356
publications.iodp.org

FINAL

doi:10.14379/iodp.proc.356.103.2017

Site U1458[1]

S.J. Gallagher, C.S. Fulthorpe, K. Bogus, G. Auer, S. Baranwal, I.S. Castañeda, B.A. Christensen, D. De Vleeschouwer, D.R. Franco, J. Groeneveld, M. Gurnis, C. Haller, Y. He, J. Henderiks, T. Himmler, T. Ishiwa, H. Iwatani, R.S. Jatiningrum, M.A. Kominz, C.A. Korpanty, E.Y. Lee, E. Levin, B.L. Mamo, H.V. McGregor, C.M. McHugh, B.F. Petrick, D.C. Potts, A. Rastegar Lari, W. Renema, L. Reuning, H. Takayanagi, and W. Zhang[2]

Keywords: International Ocean Discovery Program, IODP, Expedition 356, *JOIDES Resolution*, Site U1458, Perth Basin, Pleistocene, Houtman-Abrolhos Reef, tropical carbonates, subtropical carbonates

Contents

Background and objectives

International Ocean Discovery Program (IODP) Site U1458 lies in the northern part of the Perth Basin, 150 m from the Houtman-1 industry well on the northern Rottnest shelf (James et al., 1999; Collins et al., 2014). The site is directly seaward and downdip from the Houtman Abrolhos main reef complex, which contains the most southerly tropical reefs in the Indian Ocean. Site U1458 was the southernmost site of our latitudinal transect (Figures **F1**, **F2**, **F3**).

The evolution of this reef complex is directly related to the path of the Leeuwin Current. Dating of sediments cored at Site U1458, coupled with seismic correlation, was intended to provide insight into the pre-Quaternary history of these reefs and a long-term perspective on Leeuwin Current evolution at the tropical/subtropical boundary off Western Australia. In addition, it has been suggested that subsidence rates over the last 140 ky were low compared to those of the Carnarvon Basin reefs (Collins and Testa, 2010). Subsidence analyses of the shelf wedge drilled at this site could extend this record and allow more precise modeling of dynamic subsidence along the western margin of Australia. An additional objective was to use any finer grained facies in this section to yield a Pliocene–Pleistocene record of the onset and variability of the southern Australian winter-dominated rainfall regime.

Unfortunately, we were unable to recover the coarse-grained sediment encountered at Site U1458, and the site was abandoned in favor of alternate Site U1459, located ~1 nmi seaward and in water ~50 m deeper, where it was hoped that a finer grained section would be encountered.

Operations

Port call and initial transit to Site U1458

Expedition 356 officially began at 0800 h (UTC + 8 h) on 31 July 2015 alongside the Victoria Quay (Berth C) in Fremantle, Australia, with IODP technical staff, the Expedition Project Manager, and the Co-Chief Scientists boarding the R/V *JOIDES Resolution*. All public relations activities were concluded on 31 July. The remainder of the science party boarded the vessel on 1 August, and loading of drilling equipment, expedition stores, and food was completed. The vessel was then made ready for sea passage. On 3 August, the pilot arrived on board the ship at 1545 h, and at 1615 h the last line was released. With assistance from two harbor tugs, the vessel proceeded to the pilot station and the pilot departed the vessel at 1634 h. The 237 nmi sea voyage continued for 24.25 h and ended at the expedition's first site (U1458). The average speed for the voyage was 11.1 kt. After arriving on location at ~1400 h on 4 August, the thrusters were lowered and the dynamic positioning system was engaged. The positioning beacon was deployed and remained on the seafloor for the duration of the site. The position reference was a combination of GPS signals and a single acoustic beacon.

Site U1458

Site U1458 (28°39.8475′S, 113°34.6676′E) consisted of a single hole (U1458A). The original plan called for three advanced piston corer (APC) holes to refusal with the last two holes extended to 330 meters below seafloor with the extended core barrel (XCB) system. It became immediately apparent during operations in Hole U1458A

[1] Gallagher, S.J., Fulthorpe, C.S., Bogus, K., Auer, G., Baranwal, S., Castañeda, I.S., Christensen, B.A., De Vleeschouwer, D., Franco, D.R., Groeneveld, J., Gurnis, M., Haller, C., He, Y., Henderiks, J., Himmler, T., Ishiwa, T., Iwatani, H., Jatiningrum, R.S., Kominz, M.A., Korpanty, C.A., Lee, E.Y., Levin, E., Mamo, B.L., McGregor, H.V., McHugh, C.M., Petrick, B.F., Potts, D.C., Rastegar Lari, A., Renema, W., Reuning, L., Takayanagi, H., and Zhang, W., 2017. Site U1458. *In* Gallagher, S.J., Fulthorpe, C.S., Bogus, K., and the Expedition 356 Scientists, *Indonesian Throughflow*. Proceedings of the International Ocean Discovery Program, 356: College Station, TX (International Ocean Discovery Program).
http://dx.doi.org/10.14379/iodp.proc.356.103.2017

[2] **Expedition 356 Scientists' addresses.**

MS 356-103: Published 26 February 2017

Figure F1. Map of the northwest shelf showing major basins and location of modern and "fossil" reefs. Stars = Expedition 356 sites, green circles = Deep Sea Drilling Project/Ocean Drilling Program sites and other core locations referred to in text, yellow circles = industry well locations (Angel = Angel-1, G2/6/7 = Goodwyn-2, Goodwyn-6, Goodwyn-7, A1 = Austin-1, M/MN1 = Maitland/Maitland North-1, TR1 = West Tryal Rocks-1). WA = Western Australia, NT = Northern Territory, SA = South Australia, QLD = Queensland, NSW = New South Wales).

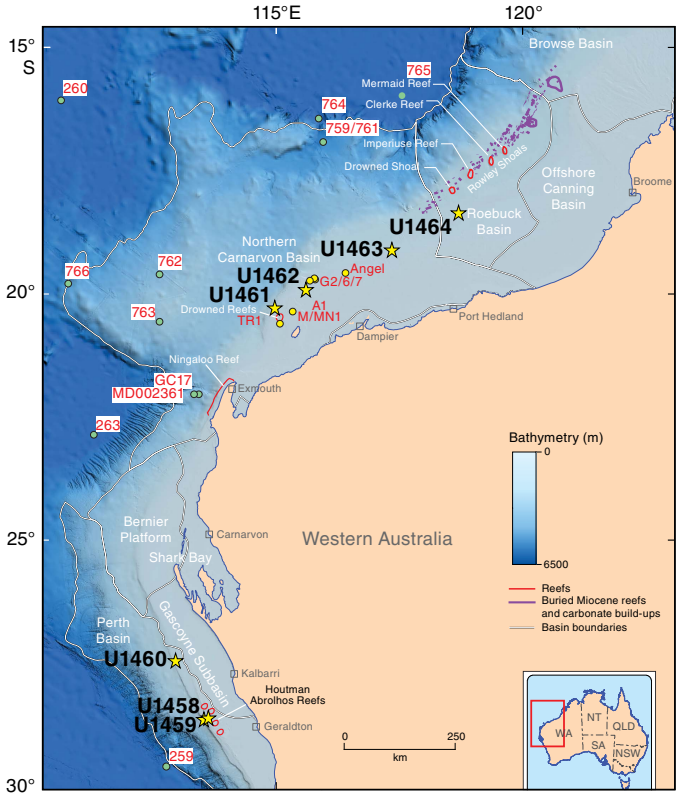

that the APC system would not penetrate the surface formation. After two attempts with the APC system, one with the XCB system, and one with the half-length APC (HLAPC) system, coring was abandoned at Site U1458. Preparations were then made to proceed to a deeper alternate site. The total time spent on Site U1458 was 1.01 days (4–5 August 2015).

A total of four cores were recorded for the site, penetrating to a total depth of 10 m drilling depth below seafloor (DSF) (Tables **T1**, **T2**). Cores 356-U1458A-1H and 2H recovered 1.05 and 2.12 m of material, respectively. Core 3X recovered no material, and Core 4F recovered only 0.55 m. Because we advanced by recovery, the overall recovery for Site U1458 was 37%.

Hole U1458A

After arriving on location, the APC/XCB bottom-hole assembly was picked up and assembled then run into the hole; there were no significant operational problems running the drill string into the hole. The top drive was picked up and spaced out and a wiper pig was inserted into the drill string. The wiper pig was pumped through the drill string with 1.5× the annular volume to clean any rust or debris from the inside of the drill string. The calculated precision depth recorder (PDR) depth for the site was 159.4 meters below sea level (mbsl). Nonmagnetic core barrels were dressed with core liners in preparation for spudding Hole U1458A. On the first core barrel run, the coring line failed. Fortunately the break was between the crown and the top drive and we were able to secure both ends. The wireline and core barrel were then T-barred back to the surface and the core barrel was recovered. The core line was then restrung and ~700 m of core line was slipped and cut from the coring winch drum. The parted coring line resulted in ~6 h of nonoperational time. We then prepared again to start Hole U1458A. The core barrel was retrieved after shooting the core, and although there was evidence that the core barrel had slightly penetrated the seafloor, no core was recovered. Hole U1458A was finally spudded at 0300 h on 5 August. The mudline core recovered 1.05 m and the seafloor was calculated to be 156.7 mbsl. Orientation was attempted starting with Core 356-U1458A-1H. At 3.1 m DSF, the formation became too hard to piston core; an XCB core barrel was dropped and a 6.3 m interval was cored without any recovery (Core 3X). The HLAPC core barrel was then deployed and recovered only 0.55 m of core. After experiencing high torque and a stuck pipe during connections, the decision was made to abandon Site U1458 in favor of an alternate site (U1459). The coring equipment was rigged down and the top drive was set back. The acoustic positioning beacon was recovered at 1415 h and the rig was secured for a 1 nmi transit using the dynamic positioning system to Site U1459. Hole U1458A concluded at 1425 h.

Figure F2. Bathymetric map showing the seafloor around Sites U1458 and U1459. Bathymetric data are derived from the Geoscience Australia Australian bathymetry and topography grid, June 2009. The positions of multichannel seismic profiles are shown. The Houtman Abrolhos reef complex is the most southerly reef system in the Indian Ocean. Red circles = locations of preexisting industry wells.

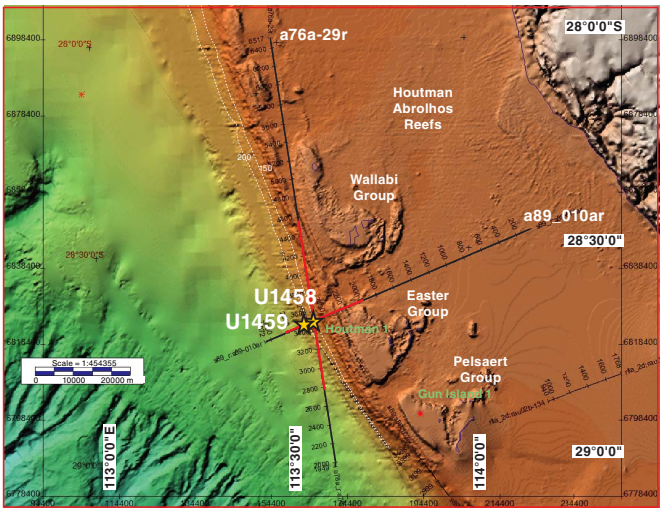

Lithostratigraphy

Site U1458 yielded a total of ~3.8 m of material (see Table **T2**). The material recovered in all cores was normally graded because of sorting of the sediment within the core liner during recovery. The poor recovery and potential reworking of sediments limited information for defining lithologic units, so only lithology is described.

Hole U1458A core material suggests a hard seafloor comprising a ~10 cm thick lithified layer with a soft-sediment cover in the mudline sample. The sediment below the lithified layer is composed of unlithified skeletal grain- to rudstone containing coarse rhodolith-bearing gravel to fine-grained carbonate sand. Diverse macro- and microfossil assemblages were found in diminishing order of abundance: rhodoliths, mollusk fragments, bryozoans, calcareous and si-

Figure F3. Multichannel seismic profile across Sites U1458 and U1459. Top of green shading = intended depth of penetration and is of Eocene age. SP = shotpoint.

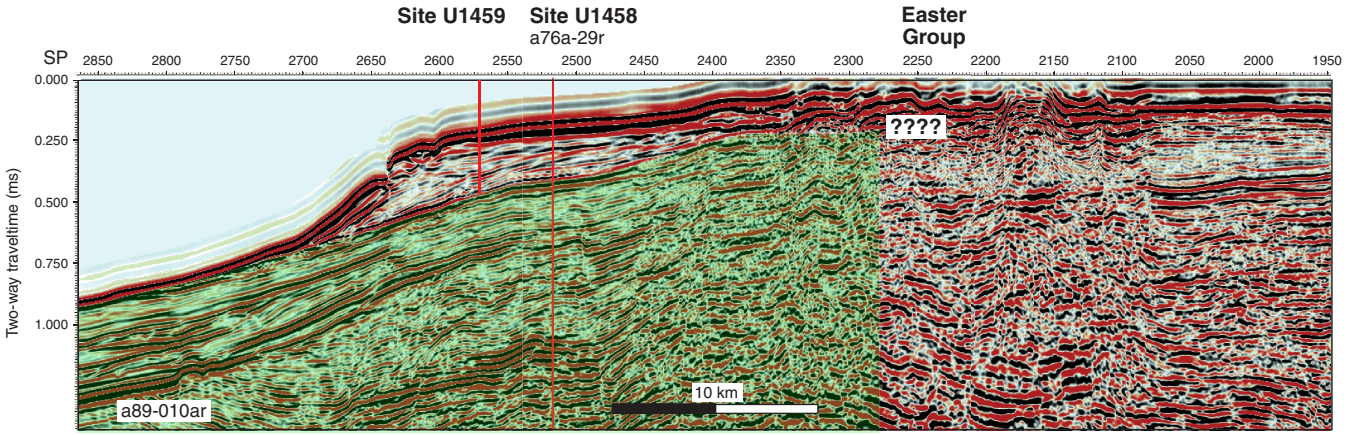

Table T1. Operations summary, Site U1458. mbsf = meters below seafloor. — = not applicable. **Download table in .csv format.**

Hole	Latitude	Longitude	Water depth (mbsl)	Penetration (mbsf)	Cored interval (m)	Core recovered (m)	Recovery (%)	Total cores (*N*)	APC cores (*N*)	HLAPC cores (*N*)	XCB cores (*N*)	RCB cores (*N*)	Time on hole (days)	Comments
U1458A	28°39.8475′S	113°34.6676′E	156.70	10.00	10.00	3.72	37	4	2	1	1	—	1.01	Hole abandoned due to low core recovery
				Totals:	10.00	3.72		4	2	1	1	—		

Table T2. Site U1458 core summary. DSF = drilling depth below seafloor, CSF = core depth below seafloor. H = advanced piston corer, X = extended core barrel, F = half-length advanced piston corer. **Download table in .csv format.**

Core	Top depth drilled DSF (m)	Bottom depth drilled DSF (m)	Advanced (m)	Recovered length (m)	Curated length (m)	Top depth cored CSF (m)	Bottom depth recovered CSF (m)	Recovery (%)	Date (2015)	Time on deck UTC (h)
356-U1458A-										
1H	0.00	1.00	1.0	1.05	1.05	0.00	1.05	105	4 Aug	1910
2H	1.00	3.10	2.1	2.12	2.12	1.00	3.12	101	4 Aug	2100
3X	3.10	9.40	6.3	0.00	0.00	3.10	9.40	0	5 Aug	0055
4F	9.40	10.00	0.6	0.55	0.55	9.40	9.95	92	5 Aug	0425

liceous sponge spicules, and benthic and planktonic foraminifers. Smear slide analyses indicate that the rudstones are predominantly composed of skeletal fragments of mollusks and bryozoan colonies. The occurrence of well-rounded to ellipsoidal gravel to coarse sand indicates moderate energy currents in the area.

Lithology (no lithostratigraphic unit defined)

Interval: 356-U1458A-1H-1A, 0 cm, through 4F-CC, 15 cm
Depth: Hole U1458A = 0–9.95 m core depth below seafloor (CSF-A)
Age: reworked Neogene containing mid-Pleistocene and Miocene nannoplankton assemblages
Lithology: grainstone to rudstone with rhodoliths

In total, four cores were recovered from Hole U1458A: 356-U1458A-1H, 2H, 3X (0% recovery), and 4F. Cores 1H and 2H contain rudstones with rhodoliths. The upper 10 cm of material in these two cores is lithified. Core 4F contains grainstone with rhodoliths. Normal grading was observed in Cores 1H, 2H, and 4F (from base to top of the core), most likely due to sorting and deformation during core recovery. The rudstone is creamy gray to beige containing abundant macrofossils. The fossils include rhodoliths, bryozoans, small and large benthic foraminifers, gastropods, and bivalves. Similar fossil assemblages were observed in Core 4F.

Smear slide description

The majority of sediments from Site U1458 were too coarse to generate smear slides, and only three were prepared. The first smear slide was taken from the mudline and is composed of 80% micrite with 15% silt-sized biogenic carbonate (Figure **F4**). The fossil assemblage in the slide is dominated by sponge spicules with lesser amounts of foraminifers, tunicate spicules, and calcareous nannoplankton. The second smear slide was taken from Sample 356-U1458A-1H-1W, 10 cm. Skeletal bioclasts compose 95% of the material. Sponge spicules, bryozoans, and echinoids accounted for the remaining 5%. The third smear slide was taken from Sample 356-U1458A-4F-1W, 4 cm. The smear slide shows a mixture of skeletal sand (70%) and silt (20%) with micrite (10%). Bryozoan fragments with lesser amounts of foraminifers and sponge and tunicate spicules dominate the fossil assemblages.

Figure F4. Photomicrograph showing a representative section of the mudline smear slide taken in Hole U1458A under transmitted light. Image width is ~4 mm. Image shows the high amount of micrite with silt-sized spicules of sponges and tunicates. Benthic foraminifers are also present, although they are relatively rare.

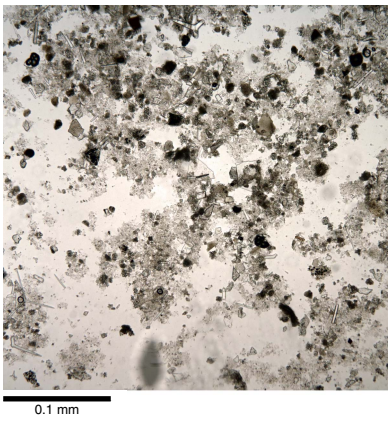

Biostratigraphy and micropaleontology

For micropaleontological analyses, a total of four samples were processed and analyzed from Hole U1458A. The material in the three core catchers (356-U1458A-1H-CC, 2H-CC, and 4F-CC) contained mostly coarse (centimeter to decimeter scale) calcareous gravel with small amounts of finer sediment and affected by coring disturbance. The fine-grained carbonate mud from the mudline was analyzed for calcareous nannofossils and stained with rose bengal to identify recently living foraminifers. See Table **T3** for details on the biostratigraphic datums determined from calcareous nannofossils and planktonic foraminifers.

Calcareous nannofossils

Calcareous nannofossils were observed in all samples, but their abundance was low. Preservation ranged from good (Sample 356-U1458A-1H-CC) to moderate–poor (Samples 2H-CC and 4F-CC). The assemblages retrieved from Samples 1H-CC and 2H-CC revealed typical recent–Pleistocene species (*Emiliania huxleyi* and/or *Gephyrocapsa oceanica*) and the presence of *Helicosphaera carteri, Braarudosphaera bigelowii, Calciosolenia* sp., and *Umbilicosphaera* spp., mixed with common, likely reworked, Neogene placolith-bearing taxa (e.g., *Reticulofenestra haqii*). Scanning electron microscope (SEM) analysis confirmed the presence of *E. huxleyi* in the mudline sample (Section 1H-1; Figure **F5**), placing this core within nannofossil Biozone NN21/CN15 (<0.29 Ma). The other cores (2H and 4F) contained mainly gephyrocapsids with a dominance of *Gephyrocapsa caribbeanica* (3–4 µm) in Core 4F, indicating material of Pleistocene age, <1.73 Ma (Biozone NN19/CN13b or CNPL8 of Backman et al., 2012).

Planktonic foraminifers

The overall species diversity was low, with five or six different taxa. Preservation varied greatly, as did the percentage of planktonic foraminifers. The following species were encountered at Site U1458: *Neogloboquadrina dutertrei, Globigerinoides ruber* (white), *Globigerinoides sacculifer* (without sac), *Globorotalia crassaformis, Globorotalia tosaensis, Globorotalia menardii*, and *Globigerinoides conglobatus* (Table **T4**).

Table T3. Calcareous nannofossil (CN) and planktonic foraminifer (PF) datums, Site U1458. Ages are according to Gradstein et al. (2012). **Download table in .csv format.**

Core, section	Depth CSF-A (m)	Marker species	Type (CN/PF)	Age (Ma)
356-U1458A-				
1H-CC	1.05	*E. huxleyi*	CN	<0.29
2H-CC	3.12	*G. tosaensis*	PF	>0.61
4F-CC	9.95	*Gephyrocapsa* spp. (>4 µm)	CN	>1.73

Figure F5. SEM photomicrograph, mudline (356-U1458A-1H-1). A. Recent–Pleistocene placoliths and calcareous sponge spicules. B. Close-up (see inset in A) of *Gephyrocapsa oceanica* (top) and *Emiliania huxleyi* (center and right).

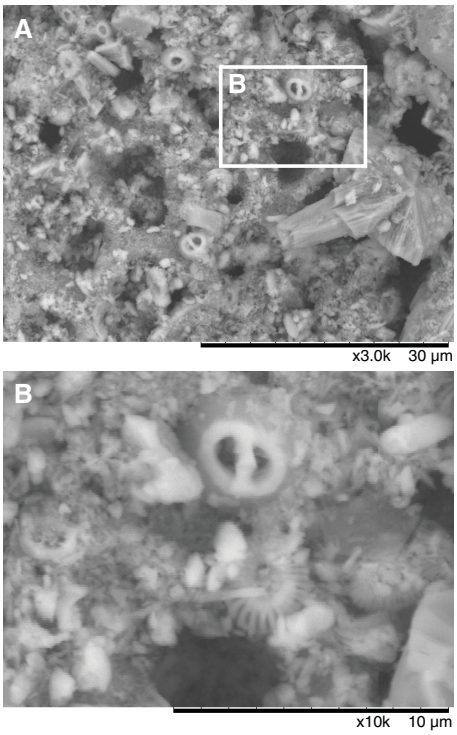

The topmost sample (356-U1458A-1H-CC) contained 12% planktonic foraminifers (PFs) with low fragmentation. This was followed by 66% PFs in Sample 2H-CC with moderate fragmentation, of which ~10% were reworked (mostly *G. sacculifer* without sac). Sample 4F-CC contained <40% PFs, of which ~10% were reworked. Preservation was poor, and there was evidence of diagenesis and inorganic precipitation or recrystallization. One key species, *G. tosaensis*, was identified in Sample 2H-CC. The top of *G. tosaensis* is reported to be at ~0.61 Ma (Gradstein et al., 2012). The specimens of this species did not appear to be reworked.

Benthic foraminifers

The samples contained between 35% and 80% benthic foraminifers with abundant warm to temperate sublittoral taxa including *Quinqueloculina lamarckiana, Quinqueloculina* spp., *Amphistegina lessonii, Cibicidoides* spp., *Cibicides* spp., and *Pullenia* spp. Between 11 and 23 species were identified in each sample (Table **T4**). Assemblage diversity decreased with depth, and dominance shifted from

Table T4. Occurrence of the main genera and species of benthic and planktonic foraminifers and additional bioclasts and minerals, Site U1458. Preservation: P = poor, G = good. Paleodepth estimates are based on calculations from van Hinsbergen et al. (2005). **Download table in .csv format.**

			Benthic foraminifers						Planktonic foraminifers		Other								
Core, section	Top depth CSF-A (m)	Bottom depth CSF-A (m)	Preservation	Benthic foraminifers/total foraminifers (%)	Planktonic foraminifers/total foraminifers (%)	Paleodepth estimate %*P* (m)	Total number of benthic species	Most abundant benthic foraminifer species (descending order)	Most frequent planktonic foraminifer species	Biozone (Gradstein et al., 2012)	Glauconite	Pyrite	Sponge spicules	Ostracods	Pteropods	Fish teeth	Bryozoans	Comment
356-U1458A-																		
1H-LIQ	0	0	G	32	68		43	*Cymbaloporetta* sp. 1; *Discorbinella* spp.; *Miliolinella* sp. 1										Mudline core top sample by APC, radiolarians, worm casings
1H-CC	1	1.05	P	88	12	50	23	*Amphistegina lessonii; Elphidium macellum; Heterolepa bradyi*	*G. ruber, G. sacculifer, N. dutertrei, G. menardii*	Pt1b			X	X	X		X	
2H-CC	3.07	3.12	P	35	65	455	16	*Heterolepa bradyi; Quinqueloculina lamarckiana; Amphistegina lessonii; Cibicides* spp.	*G. ruber, G. sacculifer, N. dutertrei, G. menardii, G. tosaensis*	Pt1a					X			
4F-CC	9.9	9.95	P	55	45	198	12	*Cibicidoides* spp.; *Pullenia* spp.; *Quinqueloculina* spp.	*G. ruber, G. sacculifer, N. dutertrei, G. menardii*	Pt1a					X		X	Strong encrustation

A. lessonii to *Q. lamarckiana*. Large benthic foraminifers accounted for between 10% and 35% of the benthic assemblage (also decreasing with depth).

It is unclear whether the shallow-water specimens are autochthonous or whether they have been transported downslope. Preservation also deteriorated with depth with few pristine specimens frequently encrusted with calcite.

Other microfossils

Other fossil groups present included ostracods (2%–3%), bryozoans (present only in Sample 356-U1458A-4F-CC), sponge spicules, and pteropods (~10%).

Geochemistry

At Site U1458, three samples were analyzed for headspace gas content (Table **T5**); all subsurface methane values were <2.5 parts per million by volume (ppmv). No other geochemical measurements were made.

Paleomagnetism

Because of the lack of recovered cores, we did not conduct any paleomagnetic or rock magnetism measurements for Site U1458.

Physical properties

Physical properties measurements at Site U1458 were collected using the Whole-Round Multisensor Logger (WRMSL), Natural Gamma Radiation Logger (NGRL), *P*-wave velocity caliper, and discrete sampling (Figures **F6**, **F7**). Gamma ray attenuation (GRA) bulk density averaged 1.33 g/cm^3 in Cores 356-U1458A-1H and 2H and 1.59 g/cm^3 in Core 4F. The average magnetic susceptibility (MS) was 0.66 SI, and two peaks were observed at 1.1–1.4 and 9.5–9.7 m CSF-A. Low natural gamma radiation (NGR) counts and low GRA bulk density occur together and correspond to the coarser rudstone, with the reverse true for the carbonate sand. These trends may be due to lithologic variations or to loss of water in the pore spaces of the coarser material. *P*-wave velocity measurements were performed on the sandier portions of Cores 1H, 2H, and 4F and fluctuated between 1500 and 1800 m/s. Color reflectance was measured on the archive halves of split cores and did not show any clear trends. One discrete sample was taken for moisture and density (MAD) analysis in each of Cores 1H, 2H, and 4F. The MAD bulk density measurements were consistent with GRA bulk density at the locations of the discrete samples. The three MAD grain density measurements range between 2.73 and 2.80 g/cm^3, and thus show essentially no differences downcore. Cores 1H and 2H have higher porosity (~55%) than Core 4F (47%).

Table T5. Headspace gas contents, Site U1458. **Download table in .csv format.**

Gamma ray attenuation bulk density

GRA bulk density averaged 1.33 g/cm^3 in Cores 356-U1458A-1H and 2H and 1.59 g/cm^3 in Core 4F. GRA bulk density tended to be relatively high at the top of each core and decreased with depth. It is possible that this trend may be due to loss of water in the pore

Figure F6. Color reflectance ratios (L*, a*, and b*, see **Physical properties** in the Expedition 356 methods chapter [Gallagher et al., 2017] for definition), Special Task Multisensor Logger (STMSL) (red) and WRMSL (black) MS, Section Half Multisensor Logger (SHMSL) point magnetic susceptibility (MSP), and NGR results, Site U1458. cps = counts per second.

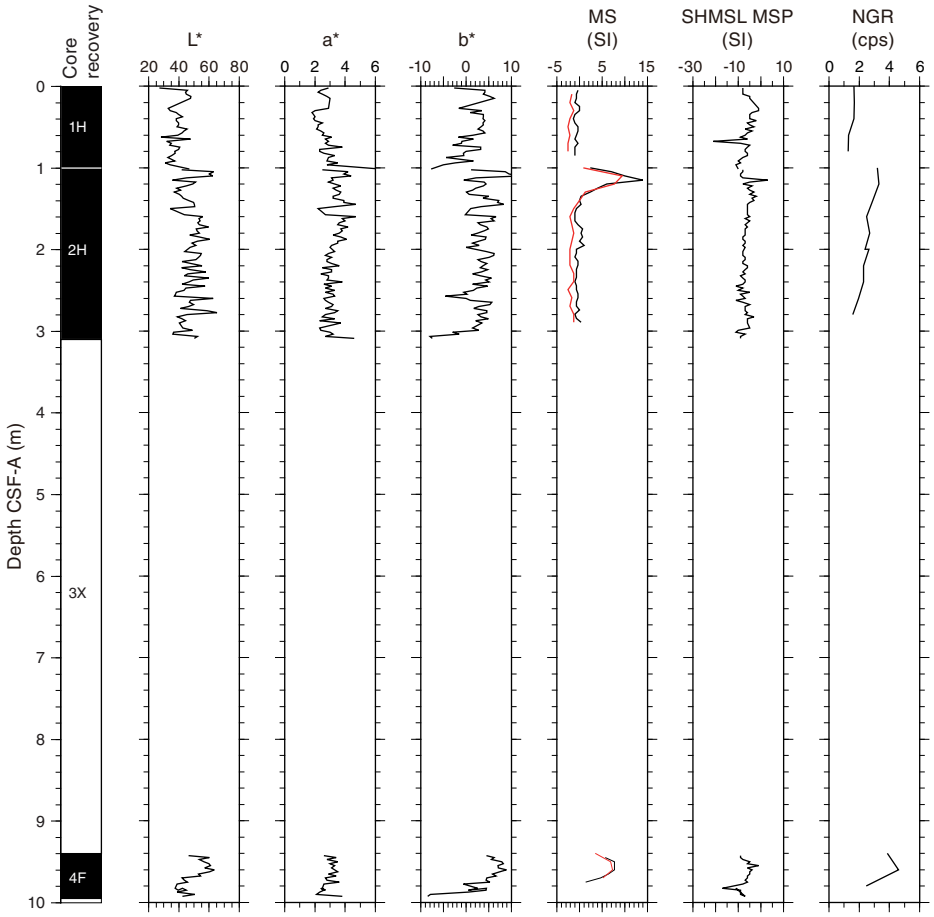

spaces of the coarser material or coring disturbance (see **Lithostratigraphy**). The maximum density (2.231 g/cm^3) occurred at 1.1 m CSF-A and corresponds to a lithified cemented rudstone.

Magnetic susceptibility

The average MS, as measured on the WRMSL, was 0.66 SI. The maximum MS (14.00 SI) occurred at 1.15 m CSF-A. A second peak in MS (7.67 SI) occurred between 9.5 and 9.7 m CSF-A. Both peaks correspond to cemented lithified rudstones.

MS was measured a second time on the archive halves (point magnetic susceptibility [MSP]). These measurements were taken at the fast and low precision (one individual measurement) instrument setting, corresponding to measurement times of about 1 s. This setting resulted in poor data resolution that cannot be compared to the WRMSL data.

Natural gamma radiation

NGR averaged 2.430 counts/s. NGR radiation tended to be relatively high at the top of each core and decreased gradually with depth. It is possible that this trend may be due to loss of water in the pore spaces of the coarser materials or coring disturbance (see **Lithostratigraphy**). The maximum NGR (4.605 counts/s) occurred at 9.6 m CSF-A and corresponds to a lithified cemented rudstone. A lesser maximum (3.308 counts/s) is observed at the top of Core 356-U1458A-2H (1.2 m CSF-A) and also corresponds to a lithified cemented rudstone.

P-wave velocity

Although *P*-wave velocity was measured on the WRMSL, the results were outside the accepted range of error. Three discrete measurements carried out with the *P*-wave caliper on the sandy units range from 1509 to 1789 m/s. The wide range of results is consistent with poor data quality and do not reflect depositional characteristics.

Moisture and density

One discrete MAD sample was taken in each of the following cores: 356-U1458A-1H, 2H, and 4F. MAD bulk density measurements were consistent with GRA bulk density measurements at the discrete sample locations and ranged from 1.79 to 1.94 g/cm^3. The three MAD grain density measurements range between 2.73 and 2.80 g/cm^3 and thus show essentially no differences downcore. Cores 1H and 2H have higher porosity (~55%) than Core 4F (47%).

Figure F7. GRA bulk density (red = STMSL, black = WRMSL, open square = MAD), *P*-wave velocity, grain density, and porosity, Site U1458.

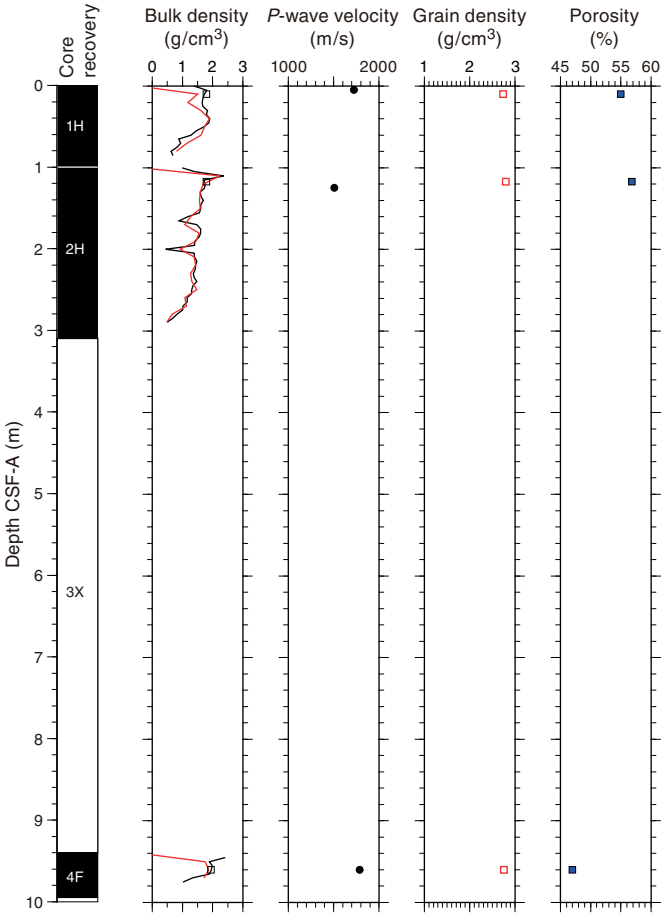

Reflectance spectroscopy and colorimetry

Color reflectance was measured on the archive halves of split cores. Reflectivity averaged 46.6% and was characterized by a standard deviation of 8.4%. The highest reflectance (up to 65.2%) corresponds to the lithified cemented rudstones. The a* values averaged 3.05, with a standard deviation of 0.59. The b* values were more variable with an average of 3.37 and a standard deviation of 2.81.

Downhole measurements

No logging was attempted at this site.

Stratigraphic correlation

No correlation was possible due to lack of material.

References

Backman, J., Raffi, I., Rio, D., Fornaciari, E., and Pälike, H., 2012. Biozonation and biochronology of Miocene through Pleistocene calcareous nannofossils from low and middle latitudes. *Newsletters on Stratigraphy,* 45(3):221–244. **http://dx.doi.org/10.1127/0078-0421/2012/0022**

Collins, L.B., James, N.P., and Bone, Y., 2014. Carbonate shelf sediments of the western continental margin of Australia. *In* Chiocci, F.L., and Chivas, A.R. (Eds.), *Continental Shelves of the World: Their Evolution During the Last Glacio-Eustatic Cycle.* Memoirs - Geological Society of London, 41:255–272. **http://dx.doi.org/10.1144/M41.19**

Collins, L.B., and Testa, V., 2010. Quaternary development of resilient reefs on the subsiding Kimberley continental margin, northwest Australia. *Brazilian Journal of Oceanography,* 58(SPE1):67–77. **http://dx.doi.org/10.1590/S1679-87592010000500007**

Gallagher, S.J., Fulthorpe, C.S., Bogus, K., Auer, G., Baranwal, S., Castañeda, I.S., Christensen, B.A., De Vleeschouwer, D., Franco, D.R., Groeneveld, J., Gurnis, M., Haller, C., He, Y., Henderiks, J., Himmler, T., Ishiwa, T., Iwatani, H., Jatiningrum, R.S., Kominz, M.A., Korpanty, C.A., Lee, E.Y., Levin, E., Mamo, B.L., McGregor, H.V., McHugh, C.M., Petrick, B.F., Potts, D.C., Rastegar Lari, A., Renema, W., Reuning, L., Takayanagi, H., and Zhang, W., 2017. Expedition 356 methods. *In* Gallagher, S.J., Fulthorpe, C.S., Bogus, K., and the Expedition 356 Scientists, *Indonesian Throughflow.* Proceedings of the International Ocean Discovery Program, 356: College Station, TX (International Ocean Discovery Program). **http://dx.doi.org/10.14379/iodp.proc.356.102.2017**

Gradstein, F.M., Ogg, J.G., Schmitz, M.D., and Ogg, G.M. (Eds.), 2012. *The Geological Time Scale 2012:* Amsterdam (Elsevier).

James, N.P., Collins, L.B., Bone, Y., and Hallock, P., 1999. Subtropical carbonates in a temperate realm; modern sediments on the southwest Australian shelf. *Journal of Sedimentary Research,* 69(6):1297–1321. **http://dx.doi.org/10.2110/jsr.69.1297**

van Hinsbergen, D.J.J., Kouwenhoven, T.J., and van der Zwaan, G.J., 2005. Paleobathymetry in the backstripping procedure: correction for oxygenation effects on depth estimates. *Palaeogeography, Palaeoclimatology, Palaeoecology,* 221(3–4):245–265. **http://dx.doi.org/10.1016/j.palaeo.2005.02.013**

Author/s:
Gallagher, SJ; Fulthorpe, CS; Bogus, K; Auer, G; Baranwal, S; Castañeda, IS; Christensen, BA; De Vleeschouwer, D; Franco, DR; Groeneveld, J; Gurnis, M; Haller, C; He, Y; Henderiks, J; Himmler, T; Ishiwa, T; Iwatani, H; Jatiningrum, RS; Kominz, MA; Korpanty, CA; Lee, EY; Levin, E; Mamo, BL; McGregor, HV; McHugh, CM; Petrick, BF; Potts, DC; Rastegar Lari, A; Renema, W; Reuning, L; Takayanagi, H; Zhang, W

Title:
Site U1458

Date:
2017

Citation:
Gallagher, S. J., Fulthorpe, C. S., Bogus, K., Auer, G., Baranwal, S., Castañeda, I. S., Christensen, B. A., De Vleeschouwer, D., Franco, D. R., Groeneveld, J., Gurnis, M., Haller, C., He, Y., Henderiks, J., Himmler, T., Ishiwa, T., Iwatani, H., Jatiningrum, R. S., Kominz, M. A. ,... Zhang, W. (2017). Site U1458. International Ocean Discovery Program.